Lifetime of Bubble Rafts: Cooperativity and Avalanches

Hernán Ritacco,* Flavien Kiefer, and Dominique Langevin
Laboratoire de Physique des Solides, Université Paris XI, 91405 Orsay, France
(Received 24 July 2006; published 14 June 2007)

We have studied the collapse of pseudo-bi-dimensional foams. These foams are made of uniformly sized soap bubbles packed in an hexagonal lattice sitting at the top of a liquid surface. The collapse process follows the sequence: (1) rupture of a first bubble, driven by thermal fluctuations and (2) a cascade of bursting bubbles. We present a simple numerical model which captures the main characteristics of the dynamics of foam collapse. We show that in a certain range of viscosities of the foaming solutions, the size distribution of the avalanches follows power laws as in self-organized criticality processes.

DOI: 10.1103/PhysRevLett.98.244501 PACS numbers: 47.55.df, 45.70.Ht, 47.57.Bc, 89.75.Da

Liquid foams are out-of-equilibrium systems. Three processes are always present and occur simultaneously: drainage (liquid drains out of the foam), coarsening (bubbles change in size by gas diffusion due to differences in capillary pressure between them), and collapse (liquid films between adjacent bubbles break); drainage and coarsening being better understood than foam collapse [1]. Drainage reduces the films thickness and, as a consequence, their stability against thermal fluctuations. It is accepted that foam collapse depends mainly on the properties of single films and the main experimental and theoretical effort was directed to the study of the rupture of isolated, single liquid films in simple geometries (planar and cylindrical films). The general idea is that films break by spontaneous growth of thermal fluctuations of film thickness. Vrij [2] proposed a model for the amplification of thermal thickness fluctuations. These fluctuations are controlled by two contributions to the free energy of the film. The first one is always positive due to the increase of the film surface area (the surface energy is the product of surface area by the surface tension γ) and the second one may be positive or negative depending on the sign of $d\Pi/dh$, Π being the disjoining pressure (force between film surfaces per unit area) and h the film thickness. The film thickness can be written as $h = h_0 + \sum_q A_q \exp(iq_x x + q_y y)$, where h_0 is the average thickness of the film and A_q is the amplitude of the fluctuation of wave vector q, $A_q(t) = A_q(0)\exp(t/\tau)$. When $\frac{d\Pi}{dh} > 0$ the characteristic time τ is positive, depends on q and presents a minimum (i.e., a maximum in the growing rate) given by

$$\tau_m = \frac{24\gamma\eta}{h_0^3}\left(\frac{d^2\Pi}{dh^2}\right)_0^{-2}, \quad (1)$$

where η is the bulk viscosity and the index "0" indicates that the derivative is calculated at h_0. If only van der Waals forces are present, the characteristic time is $\tau_m = 96\pi^2\gamma\eta h_0^5 A_H^{-2}$, where A_H is the Hamaker constant. For typical values ($\gamma = 30$ mN/m, $\eta = 1$ mPa $\cdot$ s, $h_0 = 40$ nm and $A_H = 10^{-20}$ J) $\tau_m \sim 30$ seconds. The lifetime of the film, t_{lf}, depends on h_0 and τ_m:

$$t_{lf} = \tau_m f(h_0, \gamma), \quad (2)$$

where f is a weak function of surface tension and thickness. Since, in practice, repulsive forces are frequently present, an energy barrier must be overcome. This is possible if surface density fluctuations occur, these being governed by surface elasticity ϵ: t_{lf} depends then not only on h_0, η, and Π, but also on ϵ [3].

The link between the spontaneous rupture of a single film and the collapse of a real foam is not direct because several important phenomena are not considered, among them, the influence of a bubble rupture in the breaking of neighboring films and bubbles. When a bubble breaks, part of its energy is transferred to the neighboring bubbles inducing mechanical fluctuations which can lead to other ruptures in a cascade process [4–6]. Here we go beyond studies of films by using single layers of bubbles of the same size and packed in an hexagonal lattice at the surface of a surfactant solution. Because all the bubbles have the same size, we avoid coarsening. Drainage is also suppressed because the bubbles are in contact with the bulk liquid. We avoid evaporation and dust by enclosing the system in a atmosphere saturated with liquid vapor. The surfactant solutions are poured into a glass container of 15 cm diameter and 1 cm depth. The bubble raft is formed directly above the liquid with a needle connected to an air pump. We follow the evolution of the number of bubbles with a CCD camera. The images are analyzed with software (IMAGEJ) that allows us to count bubbles and to measure their sizes (in order to check that it does not change with time). We used also a fast camera (VDS HCC-1000) able to take up to 2500 frames per second, in order to visualize the rupture of single bubbles and its influence on their neighbors.

We have used the surfactant sodium dodecyl sulfate (SDS-Sigma-Aldrich) and varied the solution viscosity by mixing water with different amounts of glycerol (Aldrich). The SDS concentration used is 15 mM, twice the critical micellar concentration. All the solutions have a similar surface tension, $\gamma \sim 30$ mN/m and surface elasticity [7]. The measurements were made at room temperature on rafts composed of 400 ± 50 bubbles and repeated a minimum of 20 times (the less viscous systems were measured up to 200 times).

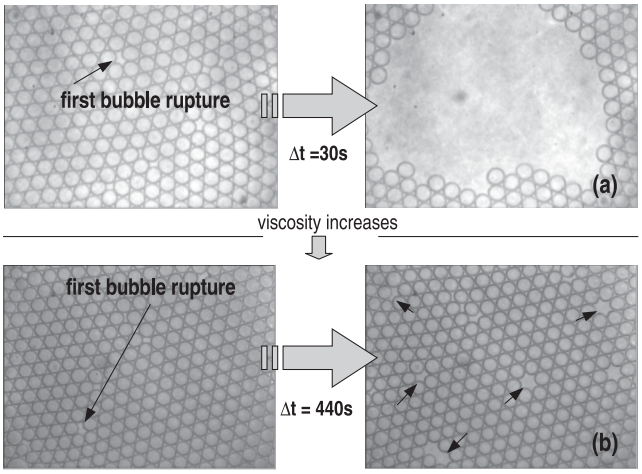

FIG. 1. Time evolution of bubbles rafts. (a) $\eta = 1$ mPa · s; the first bubble rupture produces an avalanche which destroys all the raft in 30 s; (b) $\eta = 2.6$ mPa · s; bubbles burst almost independently each other (arrows). Here the total time for the complete destruction of the raft is several hours.

Figure 1 shows typical snapshots taken at different times. Without glycerol, when the first bubble bursts, it produces a perturbation which extends to the neighboring bubbles and produces a first cascade. Other bubbles burst later and in different areas, producing further cascades and leading to the complete collapse of the bubble raft [Fig. 1(a)]. Here the process is ruled by mechanical perturbations. In the case of a water-glycerol solution of bulk viscosity 2.6 mPa · s, avalanches are rare and the bubbles burst almost independently of each other. Figure 2 shows snapshots taken with a fast CCD camera for a bursting bubble showing the deformation produced onto the neighboring bubbles. These flower shaped bubbles around a bursting one were observed before in Champagne wine [8]. Figure 3(a) shows typical results for the relative number of bubbles (N/N_0, N, and N_0 being the remaining and initial number of bubbles, respectively) as a function of time and for four different glycerol concentrations. We define characteristic times to describe the behavior of the bubbles layer: t_0 is the time after which the first bubble bursts, $t_{1/2}$ is the time elapsed between t_0 and the moment when the number of bubbles is equal to $N_0/2$, and, finally, t_f is the time elapsed between t_0 and the last bubble rupture [see Fig. 3(a)]. The characteristic time t_0 is related mainly to τ_m, i.e., with the isolated film properties. The time $t_{1/2}$ and t_f are affected by the mechanical energy liberated by the bursting of previous bubbles.

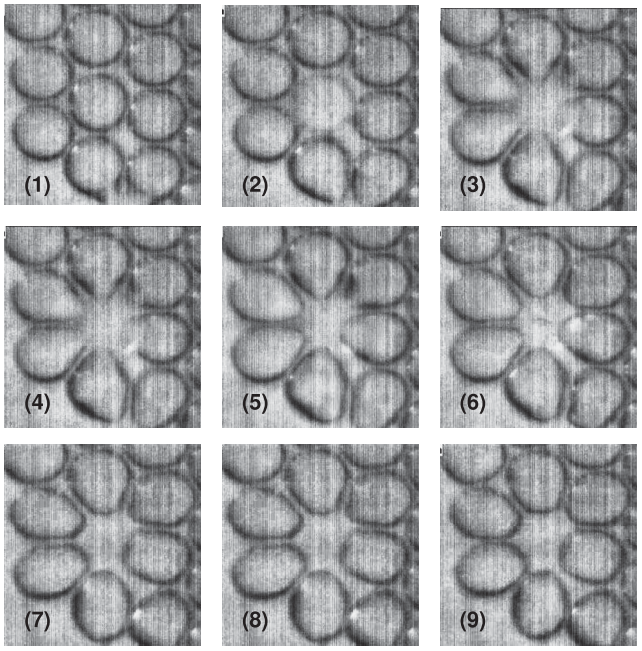

FIG. 2. A bubble rupture observed with a fast camera ($\eta_r = 2$). The total time elapsed between snapshot (1) and (9) is 0.0225 s.

The values of t_0 are hard to obtain experimentally with confidence, especially for the low glycerol contents, because they are not sufficiently larger than the time needed to prepare the bubble raft (raft production $\sim 7s$. For $\eta = 1$, $t_0 \sim 5$ s; for $\eta = 2$, $t_0 \sim 1000$ s). The time t_f is easily measured for a particular raft but the last bubbles often remain intact during a very long time and t_f is therefore not very sensitive to cooperative processes. The time $t_{1/2}$ is always well defined and describes the best cooperativity of the process; therefore, we shall use it to characterize the systems behavior. In Fig. 4(a) t_0 and $t_{1/2}$ are represented as a function of reduced bulk viscosity ($\eta_r = \eta/\eta_{\text{water}}$). The time t_0 seems to be independent of η except for very low viscosities and $t_{1/2}$ increases with bulk viscosity until $\eta_r \sim 1.2$, it plateaus up to $\eta_r \sim 2.6$ and increases afterwards. In the following, we propose a numerical model for the collapse dynamics of the bubble rafts. The justification of the model is heuristic. We used an hexagonal lattice with $N_0 = m^2$ sites. Each site is occupied by a bubble which can be in two states: broken (state "1") or intact (state "0").

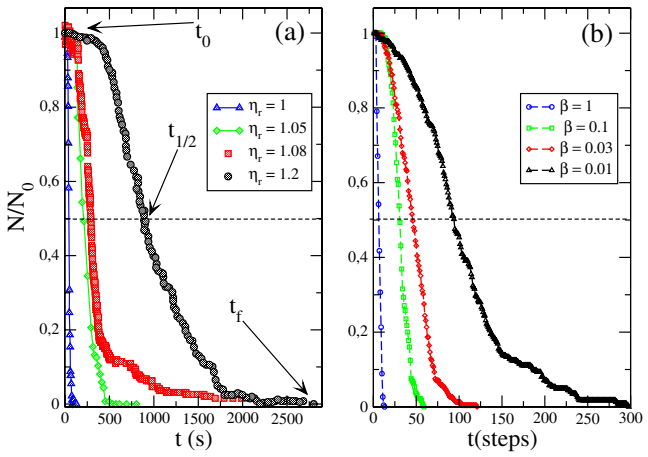

FIG. 3 (color online). (a) Time evolution of bubble rafts for four different viscosities: 1; 1.05; 1.08; 1.2 mPa · s. (b) Simulated results for $\beta = 1$; 0.1; 0.03; 0.01 in a raft of 400 bubbles ($m = 20$).

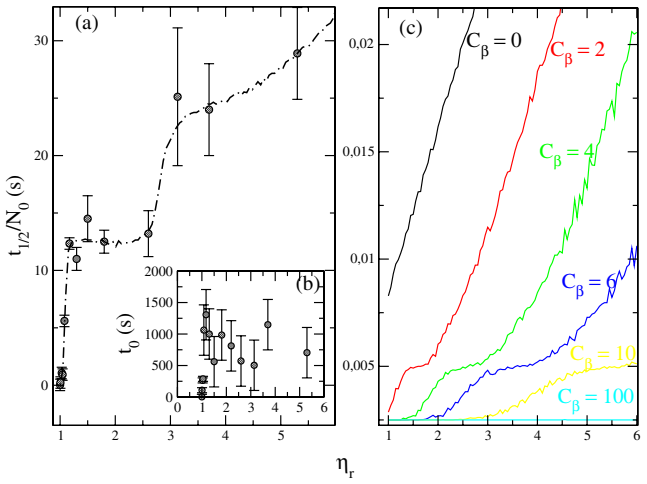

FIG. 4 (color online). Characteristic times (a) Experiment on raft composed of $N_0 \sim 400$ bubbles (b) Simulations for $m = 20$, $C_t = 6$, and C_β from 0 to 100.

We assumed that there exists a critical energy, E_c which transferred to a bubble breaks it instantaneously. For a system free of external constraints, the first bubble rupture is a random process driven by thermal fluctuations. We define the initial probability, $P_1^0 = 1/\hat{t}_{lf}$, where $\hat{t}_{lf}$ is the adimensional counterpart of t_{lf} [Eq. (2)]. When a bubble bursts, part of its energy is transferred to the neighboring bubbles (Fig. 2). The energy transferred to the six neighbors of a bursting bubble is $\Delta E_b \propto (\gamma a)$, a being the bubble surface. If ΔN_b is the number of ruptured bubbles and ΔE the energy transmitted by these bubbles to a neighbor, $\Delta E/E_c = (\beta/6)\Delta N_b$, with $\beta = \Delta E_b/E_c$. If $\Delta E/E_c > 1$ the bubble ruptures; but if $\Delta E/E_c < 1$ the bubble can or cannot rupture (they are always under the action of thermal fluctuations). Then, P_1 changes as follows:

$$P_1 = \begin{cases} P_1^0 + \frac{\beta \Delta N_b}{6} & \text{if } P_1^0 + \frac{\Delta E}{E_c} < 1 \\ 1 & \text{if } P_1^0 + \frac{\Delta E}{E_c} > 1 \end{cases}. \quad (3)$$

We used the following scheme for the simulation: we produce an hexagonal lattice of m^2 sites all in state 0. We assigned to each site the initial probability $P_1^0(i, j)$. We generated m^2 random numbers $r_{(i,j)}$ and if $r_{(i,j)} \leq P_1^0(i, j)$ we changed the site to state 1 and we change the probabilities of all the 6 neighboring sites according to Eq. (3). Then we repeated the cycle. If in a complete cycle there is no change in ΔN_b for a site in the lattice, we relaxed the probability of that site to the initial probability P_1^0. Doing that we mimic the energy dissipated by the bubble in the bulk liquid (see the evolution of the bubble oscillations in Fig. 2). In the algorithm, there is no rule that permits state 1 to go to state 0; when a bubble bursts it cannot regenerate again. For physically realistic boundary conditions that mimic the walls of the glass container we used a lattice of $(m + 2)^2$ sites enclosing our lattice of m^2 sites were the bubbles out of the internal lattice never burst. Figure 3(b) shows the results of the simulations for 4 different values of β: the resemblance with Fig. 3(a) is striking.

Let us now discuss the influence of bulk viscosity. We take for simplicity, $\beta = C_\beta/\eta_r$ (other dependences on η_r lead to similar results) and $\hat{t}_{lf} = C_t\eta_r$ [as in Eq. (1) and (2), other film rupture processes leading to similar viscosity dependences], C_β and C_t being constants. The results for $t_{1/2}$ are shown in Fig. 4(c). When $C_\beta = 0$, no energy is transferred when a bubble bursts; foam collapse is driven only by thermal fluctuations and $t_{1/2}$ increases linearly with viscosity. As C_β increases, $t_{1/2}$ increases less rapidly with viscosity until a plateau is seen as in the experimental results [compare Figs. 4(a) and 4(c)]. These plateaus arise because the time at which $n = N_0/2$ can be reached in many different ways depending on the number of simultaneous avalanches and on the ratio $\Delta E/E_c$. Let us use an example to illustrate this. Suppose that the raft is composed initially of 400 bubbles, with an initial probability $P_1^0 = 0.35$. After the first cycle of the simulation there will be approximately $400 - P_1^0 400 = 260$ bubbles. After the next cycle there will be a maximum of $260 - 91 = 169$ bubbles (we are not considering avalanches), and therefore $t_{1/2} = 2$. If we increase the viscosity, P_1^0 decreases, for example, to 0.3, there will then be $400 - 120 = 280$ bubbles after the first cycle and a maximum of 196 bubbles after the second and again $t_{1/2} = 2$. We then see how the plateau is built. If in the above example we increase again the viscosity and P_1^0 falls to 0.25, $t_{1/2}$ will increase to 3. The values of β (and C_β) affect the position and the width of the plateaus. If the energy liberated by a bursting bubble is many times greater than the energy needed to break its neighbors ($\beta \gg 1$) the increase of bulk viscosity will no affect $t_{1/2}$ because we will have always $P_1 = 1$, and there will be a long plateau [$C_\beta = 100$ in Fig. 4(c)]. If the viscosity increases enough, the energy release by a bursting bubble will be below the energy threshold, E_c, and the plateau will end.

In the simulation (for $C_\beta = 5$ and $C_t = 6$), t_0 is independent of viscosity. This is because the probability P_1^0 goes from 1/6 ($\eta_r = 1$) to 1/36 ($\eta_r = 6$), then, in a raft of 400 bubbles, there will be always (at least) one bubble rupture in the first cycle of the simulation. Note that the experimental t_0 is also constant within experimental error [Fig. 4(b)]. Let us now discuss the possible relation between foam collapse and self-organized criticality. In 1987, Bak, Tang, and Wiesenfeld introduced the self-organized criticality concept (SOC) [9,10]. SOC is based on the idea that a complex behavior can develop spontaneously in certain nonequilibrium systems with many body interactions and exhibiting abrupt changes in dynamic behavior (avalanches), the statistical distribution of events following power laws. Various complex systems follow these power laws such as light emitted from a quasar, population sizes in cities, the Gutenberg-Richter law of earthquakes, biological evolution, or forest fires [11]. Müller and di Meglio

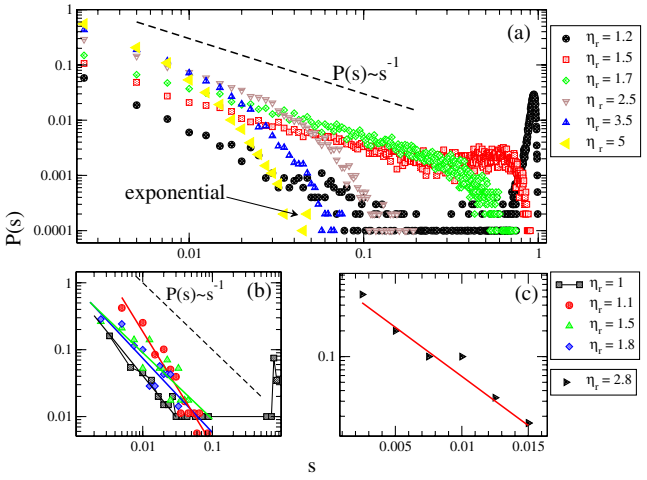

FIG. 5 (color online). (a) Simulation: Size distribution for the first avalanche simulated with the model over 10 000 runs for different viscosities ($m = 20$, $C_\beta = 3$: In these simulations only one avalanche at a time is allowed). (b) Experiment: Size distribution of the first avalanche for different viscosities (power-law behavior). (c) Experiment: Size distribution for $\eta_r = 2.8$ (exponential behavior).

[6] and Vandewalle *et al.* [4,5] have shown that the distributions of time between successive avalanches and of the energy dissipated follow power laws suggesting that 3D-draining foam collapse is a SOC dynamical process.

Here, we define an avalanche as an event of energy release (bubbles ruptures) that occurs at different positions on the raft or with a minimum time separation of $1/30$ s (camera temporal resolution); the size of an avalanche will be the number of bubbles involved in it. Figure 5 shows the size distribution of the first avalanche, $P(s)$ simulated and measured for systems of different viscosities, where $s = n/N_0$, n being the number of bubbles ruptured in an avalanche, and $P(s)$ the frequency of occurrence of an avalanche of size s divided by the total number of experiments (or runs). Simulations and experiments show the same qualitative behavior. For solutions of low bulk viscosity the power-law distribution was observed only for small avalanches in a limited range. These systems exhibit a peak for n close to the initial number of bubbles in the raft. The exponents found for the regions with power laws varies from 2.2 to 0.8. For intermediate viscosities we found power laws with an exponent of 1 ± 0.2 for a wide range of s values. For high viscosities the distribution of avalanche sizes seems to be exponential. For the very high viscosities there are no avalanches at all (at least in the limited number of experiments that we did $\sim$40).

This scenario is very similar to the case of avalanches on rice piles. Frette *et al.* carried out experiments with different types of rice [12]; rice with grains of large aspect ratio exhibit SOC behavior whereas rice with less elongated grains exhibit stretched exponential avalanche distributions. SOC behavior requires a separation of times scales: the external driving process needs to be much slower than the internal relaxation process. This is intimately related with the existence of thresholds which ensure the separation of time scales. The ability of spherical grains to roll or flow eliminates the threshold and limits the number of possible metastable configurations. We can identify all these elements in our bubble rafts. The driving force comes from thermal fluctuations and the threshold arise from the existence of a critical energy to break a bubble, E_c. If the energy communicated by a bursting bubble to its neighbors is large enough, all bubbles burst in a big avalanche because there is no threshold, as in the case of rounded grains of rice. The viscosity plays here the role of grain aspect ratio in rice piles. Bubble rafts follow SOC behavior only in a limited range of viscosities and $\Delta E/E_c$ ratios.

We are currently investigating the role of surface tension, surface elasticity, and viscosity in the time evolution of bubbles rafts. These ideas could easily be extended to 3D-foams under the same conditions (no drainage, no coarsening) and could be eventually tested in future experiments on the International Space Station. We are also currently trying to implement drainage in the simulations by adding a vertical profile in P_1^0 and E_c in order to compare with the experimental results for 3D draining foams [4,5].

The authors gratefully acknowledge the financial support of the European Space Agency (No. ESA- MAP-14914/02/NL/SH).

*ritacco@quim.ucm.es

[1] Denis Weaire and Stefan Hutzler, *The Physics of Foams* (Clarendon, Oxford, 1999).
[2] A. Vrij, Discuss. Faraday Soc. **42**, 23 (1966).
[3] D. Exerowa, D. Kashchiev, and D. Platikanov, Adv. Colloid Interface Sci. **40** 201 (1992); D. Langevin, Adv. Colloid Interface Sci. **88**, 209 (2000).
[4] N. Vandewalle, J. F. Lentz, S. Dorbolo, and F. Brisbois, Phys. Rev. Lett. **86**, 179 (2001).
[5] N. Vandewalle and J. F. Lentz, Phys. Rev. E **64** 021507 (2001).
[6] W. Muller and J.-M. di Meglio, J. Phys. Condens. Matter **11**, L209 (1999).
[7] H. Ritacco (unpublished).
[8] G. Liger-Belair and P. Jeandet, Langmuir **19**, 5771 (2003).
[9] P. Bak, C. Tang, and K. Wiesenfeld, Phys. Rev. Lett. **59**, 381 (1987).
[10] P. Bak, *How Nature Works* (Copernicus, Springer-Verlag, New York, 1996), 1st ed.
[11] H. J. Jensen, *Self-Organized Criticality: Emergent Complex Behavior in Physical and Biological Systems* (Cambridge University Press, New York, 1998).
[12] V. Frette, K. Christensen, A. Malthe-Sorenssen, J. Feder, T. Jossang, and P. Meakin, Nature (London) **379**, 49 (1996).